# Signalling pathways of an insulin-mimetic phosphoinositolglycan–peptide in muscle and adipose tissue

Alexandra KESSLER*, Günter MÜLLER†, Susanne WIED†, Anna CRECELIUS† and Jürgen ECKEL*[1]

*Department of Molecular Cardiology, Diabetes Research Institute, Düsseldorf, Germany and †Hoechst Marion Roussel Deutschland GmbH, Research Metabolism, Frankfurt, Germany

A novel phosphoinositolglycan–peptide (PIG-P) from the yeast *Saccharomyces cerevisiae* potently mimicks insulin action on glucose transport and metabolism in rat muscle and adipose tissue. The aim of the present study was to elucidate the cellular signalling pathways of this insulin-mimetic compound. Rapid onset and reversibility of PIG-P action on glucose transport were observed in isolated adipocytes with a half-time of transport stimulation of 6–8 min (insulin less than 5 min). Combined treatment with PIG-P and insulin indicated additive stimulation of glucose transport at submaximal concentrations and non-additive action of both agents at maximal doses. The tyrosine phosphorylation of insulin receptor substrate-1 (IRS-1) was markedly increased in response to PIG-P in rat cardiomyocytes without any effect on the tyrosine phosphorylation of the insulin receptor $\beta$-subunit. PIG-P action in these cells was accompanied by phosphorylation/dephosphorylation of several proteins with molecular masses of 15–30 kDa, a response not detected with insulin. Downstream signalling of IRS-1 was then analysed by monitoring IRS-1-associated phosphatidylinositol 3-kinase (PI 3-kinase) activity in cardiomyocytes. A stable (2 and 15 min incubation with PIG-P) 7-fold stimulation corresponding to about 50 % of insulin action could be detected. Increased tyrosine phosphorylation of IRS-1 and enhanced PI 3-kinase activity in response to PIG-P independent of the insulin receptor was also observed in isolated adipocytes. Involvement of PI 3-kinase in PIG-P action was subsequently confirmed by the dose-dependent inhibition of PIG-P-activated glucose transport in rat diaphragm and adipocytes by the PI 3-kinase inhibitors wortmannin and LY294002. These data suggest divergent upstream signalling by insulin and PIG-P involving phosphoproteins not affected by insulin. However, PIG-P and insulin action converge at the level of IRS-1 inducing insulin-independent PI 3-kinase-mediated signalling to glucose transport.

## INTRODUCTION

Considerable progress has been made in correlating the tyrosine kinase function of the insulin receptor to a complex network of cross-talking downstream signalling elements that finally mediate the pleiotropic effects of insulin (for reviews, see [1,2]). A major mechanism of this signalling cascade involves tyrosine phosphorylation of the insulin receptor and additional proteins such as insulin receptor substrate-1/2 (IRS-1/2), Shc and pp60 and interaction with SH2 domains of an additional set of downstream proteins [3]. Two pathways within this network have been dissected and are thought to mediate different biological functions of the hormone. (1) Activation of phosphatidylinositol 3-kinase (PI 3-kinase) by interaction of the p85 subunit with IRS-1/2 plays a pivotal role in the stimulation of glucose transport by insulin [4,5] and the regulation of cellular trafficking [6]. (2) Formation of the Shc–Grb2 complex leads to enhanced $p21^{ras}$ GTP binding and finally to activation of mitogen-activated protein kinase, an enzyme involved in both cell growth and metabolism [3]. An additional much less well-defined pathway of insulin signalling involves the activation of a specific phospholipase C [7,8] that hydrolyses glycosylphosphatidylinositol (GPI) lipids in the plasma membrane, leading to the production of soluble phosphoinositolglycan (PIG) molecules. These compounds are thought to function as second messengers of insulin action (for reviews, see [9,10]). However, molecular targets of PIG action and the precise relationship to insulin signalling has remained poorly understood.

Compositional analysis of PIG molecules suggested that they consist of a core structure of phosphoinositol, glycosidically linked to glucosamine which is coupled to an oligosaccharide of varied composition [10]. Further, the GPI lipid precursors were found to be structurally related to the GPI anchors of glycolipid-modified plasma-membrane proteins [11]. PIG molecules, the polar headgroups of GPI structures, may therefore be generated in response to insulin by lipolytic or lipolytic/proteolytic processing of the corresponding precursors [9,10]. PIG molecules can be isolated from human serum, and very recently inadequate generation of a PIG mediator in patients with non-insulin-dependent diabetes mellitus has been reported [12]. Documented effects of inositolglycans from insulin-treated cells or GPI-anchored proteins include stimulation of lipogenesis [13], inhibition of lipolysis [14], activation of pyruvate dehydrogenase and inhibition of gluconeogenesis [15].

Despite substantial evidence for insulin-regulated GPI turnover and a possible association with insulin signalling, essentially no data are at present available on the molecular targets and mechanisms of PIG action. So far, such an analysis has been prohibited by limited amounts and ill-defined structures of the different PIG preparations. This problem has recently been resolved by us by the purification of a phosphoinositolglycan–peptide (PIG-P) from yeast [16]. This PIG-P can be obtained in considerable amounts, is chemically completely defined and was found to exert a broad spectrum of insulin-like actions in muscle and adipose tissue [16]. In contrast with PIG molecules described so far, this compound potently activates glucose transport and GLUT4 translocation [16]. We therefore analysed the mechanisms of PIG-P signalling to glucose transport and compared it with insulin using primary myocytes and adipocytes. The data show that PIG-P and insulin signalling converge at the level

Abbreviations used: Gce1p, glycolipid-anchored cAMP-binding ectoprotein from *Saccharomyces cerevisiae*; GPI, glycosylphosphatidylinositol; IRS-1, insulin receptor substrate-1; PI 3-kinase, phosphatidylinositol 3-kinase; PIG-P, phosphoinositolglycan–peptide.

[1] To whom correspondence should be addressed.

of IRS-1/PI 3-kinase with different upstream signalling. It is suggested that PIG-P provides the structural requirements needed for insulin signalling independent of the insulin receptor.

## MATERIALS AND METHODS

### Materials

2-Deoxy-D-[2,6-$^3$H]glucose (45 Ci/mmol), 3-*O*-methyl-D-[U-$^{14}$C]glucose (50 mCi/mmol) and [$^{33}$P]$P_i$ (3000 Ci/mmol) were obtained from Amersham (Braunschweig, Germany). [$\gamma$-$^{32}$P]ATP (6000 Ci/mmol) was purchased from New England Nuclear (Dreieich, Germany). Collagenase was a product of Serva (Heidelberg, Germany) (for the isolation of cardiomyocytes) or Biochrom (Berlin, Germany) (Worthington CLSI; for the isolation of adipocytes). Wortmannin, rapamycin and phosphatidylinositol were supplied by Sigma (München, Germany). LY294002 was from RBI (Biotrend, Cologne, Germany), and PD098059 was provided by Hoechst Synthesis Department (Frankfurt, Germany). Anti-phosphotyrosine monoclonal antibody (4G10) and goat anti-mouse IgG–alkaline phosphatase conjugate were obtained from UBI (Lake Placid, NY, U.S.A.). Anti-IRS-1 antibody was kindly provided by Dr. Ton Maassen (University of Leiden, Leiden, The Netherlands). Agarose-coupled anti-phosphotyrosine antibody was purchased from Sigma. Anti-(insulin receptor) antibody was from Transduction (Lexington, CT, U.S.A.). Protein A and Protein G beads were supplied by Pierce (KMF, Germany). All other chemicals were of the highest analytical grade and were purchased from Sigma or Merck (Darmstadt, Germany). Normal Wistar rats were obtained from the animal breeding station of Hoechst Marion Roussel Deutschland GmbH (Kastengrund, Germany).

### Preparation and purification of PIG-P

PIG-Ps were prepared from the GPI-anchored plasma-membrane protein, Gce1p, isolated from the yeast *Saccharomyces cerevisiae* [17], by sequential lipolytic and proteolytic digestion and purified to homogeneity as described previously [16]. The precipitated Gce1p was digested with V8 protease (*Staphylococcus aureus*) under denaturing conditions. The resulting GPI–peptide was subjected to sequential gel-filtration and hydrophobic-interaction chromatography. The eluted material was digested with phosphatidylinositol-specific phospholipase C (*Bacillus cereus*). The final purification was performed by sequential gel filtration on Bio-Gel P4, anion-exchange chromatography by SAX HPLC, two successive runs on Si-60 HPTLC plates and a final Bio-Gel P4 chromatography. The purification protocol using the criteria of recovery of [$^3$H]inositol, [$^3$H]inositol-1,2-cyclic phosphate, $A_{220}$, total insulin-mimetic activity and the relative enrichment of the insulin-mimetic activity on the basis of the content of [$^3$H]inositol and $A_{220}$ strongly argued that the insulin-mimetic activity of the final preparation is based exclusively on the PIG-P. For determination of PIG-P concentration, the amount of $P_i$ (after acid hydrolysis; 2 mol/mol) and tyrosine (by amino acid analysis) was measured. The structure of PIG-P, $NH_2$-Tyr-Cys-Asn-ethanolamine-$PO_4$-6(Man1-2)-Man1-2Man1-6Man1-4Glc$NH_2$1-6*myo*-inositol-1,2-cyclic$PO_4$, compatible with the known consensus structure of yeast GPI anchors, was determined by a combination of amino acid analysis, Dionex exchange chromatography of fragments generated enzymically or chemically from the neutral glycan core, NMR spectroscopy of the complete as well as deaminated/dephosphorylated forms, gas chromatographic/mass spectral analysis after chemical or enzymic treatment, gas chromatographic analysis of the complete GPI anchor peptide generated by Pronase digestion of Gce1p and measurement of the insulin-mimetic activity left after specific chemical and enzymic cleavage within the glycan or peptide portion of the PIG-P [16]. These analyses confirmed that the PIG-P preparation used in the present study is chemically homogeneous and of defined structure.

### Isolation of rat adipocytes

Rat adipocytes were isolated as described by Rodbell [18] with the following modifications. Epididymal fat-pads obtained from male Wistar rats (140–160 g) were placed in Krebs–Ringer–bicarbonate (KRB) buffer (12 mM $KH_2PO_4$, 1.2 mM $MgSO_4$, 4.8 mM KCl, 25 mM $NaHCO_3$, 120 mM NaCl, 1.4 mM $CaCl_2$, 5 mM glucose and 2.5 % BSA, pH 7.4, gassed with carbogen). Each pad was then cut into two or three pieces. Two pieces each were incubated with 1.5 ml of digestion buffer (10 mg of collagenase in 9 ml of KRB buffer) for 15–30 min at 37 °C in a shaking water bath. Released adipocytes were finally washed three times with Krebs–Ringer–Hepes (KRH) buffer (25 mM Hepes, 80 mM NaCl, 1 mM $MgSO_4$, 2 mM $CaCl_2$, 6 mM KCl, 1 mM sodium pyruvate, 0.5 % BSA, pH 7.4) by flotation and then diluted to a final volume equal to 20 ml of KRH buffer/g of fat ($2.5 \times 10^5$ cells/ml).

### Isolation of ventricular cardiomyocytes

$Ca^{2+}$-tolerant myocytes were isolated from male Wistar rats (260–320 g) by perfusion of the heart with collagenase as previously described [19,20]. The final cell suspension was washed three times with Hepes buffer (composition: NaCl 130 mM, KCl 4.8 mM, $KH_2PO_4$ 1.2 mM, Hepes 25 mM, glucose 5 mM, BSA 20 g/l, pH 7.4, equilibrated with oxygen) and incubated in silicone-treated Erlenmeyer flasks in a rotating water bath shaker at 37 °C. After 20 min, $CaCl_2$ and $MgSO_4$ (final concentration 1 mM) were added and incubation was continued for at least 60 min until further use. Cell viability was checked by determination of the percentage of rod-shaped cells; it averaged 90–95 % under all incubation conditions. For labelling with [$^{33}$P]$P_i$, freshly prepared cardiomyocytes were incubated in phosphate-free Hepes buffer with 200 $\mu$Ci of [$^{33}$P]$P_i$/ml of cell suspension ($1 \times 10^6$ cells/ml) for 2.5 h at 37 °C followed by stimulation with insulin or PIG-P for the indicated times. Cells were then rapidly frozen in liquid nitrogen.

### Preparation of rat diaphragms

Wistar rats (60–80 g, fed *ad libitum*) were killed by decapitation, and intact diaphragms (with attached rib cage) were removed quickly (1–2 min) as described [21]. The diaphragms maintained intact their insertions to the xiphoid process, ribs, central tendon and spine and thus had all of their muscle fibres intact. The sternum was divided horizontally at the level of the fourth costal cartilage, after which the ribs were transected superior to the insertions of the diaphragm. Extraneous connective tissue, bone and muscle were trimmed away before use. The hemidiaphragms were washed once with 0.9 % NaCl and once with KRO buffer (80 mM NaCl, 6 mM KCl, 2 mM $CaCl_2$, 1 mM $MgSO_4$, 1.2 mM $KH_2PO_4$, 0.1 % BSA, 25 mM Hepes/KOH, pH 7.5, equilibrated with $O_2$) containing 5 mM glucose, blotted on filter paper and then placed in 50 ml plastic vials containing 20 ml of the same buffer.

### Assay of glucose uptake

Glucose transport in adipocytes was determined as uptake of 2-deoxy-[$^3$H]glucose as described by Foley and Gliemann [22]. Briefly, 0.4 ml of adipocytes in KRH buffer ($2.5 \times 10^5$ cells/ml)

were incubated with insulin or PIG-P as indicated in a total volume of 1 ml of KRH buffer. Initial rates of glucose transport were determined by adding 50 $\mu$l of KRH buffer containing 2-deoxy-D-[$^3$H]glucose (0.5 $\mu$Ci; 2 mM) to the incubation for 5 min and subsequent separation of 100 $\mu$l aliquots of the cells by centrifugation through 50 $\mu$l of dinonylphthalate. Preincubation of the cells with 20 $\mu$M cytochalasin B was used to correct the values for simple diffusion and non-specific trapping of the hexose. In experiments evaluating the time course of activation and reversibility, glucose transport was determined by replacing 2-deoxy-[$^3$H]glucose with 3-*O*-methyl-[U-$^{14}$C]glucose (2 $\mu$Ci; 1 mM) to allow assay periods of 5 s. Double-labelling experiments with 3-*O*-[$^3$H]methylglucose and [U-$^{14}$C]sucrose revealed that the extracellular water space accounted for 12–18 % and remained almost constant for between 5 and 45 s, indicating equilibration after the 5 s assay period. The intracellular water space was less than 1 % at 5 s. In routine experiments, entrapment of 3-*O*-methylglucose in the extracellular water space and diffusion of the sugar into the intracellular water space were corrected for using control incubations in the presence of 20 $\mu$M cytochalasin B. Under these conditions, time-course experiments demonstrated linear uptake of 3-*O*-methylglucose up to a 45 s assay period. Thus measurement of glucose uptake using 3-*O*-methylglucose and a 5 s assay period truly reflects the initial linear rate of glucose transport.

Glucose transport in diaphragms was determined by incubation of the hemidiaphragms with insulin/PIG-P in 20 ml of KRO buffer containing 5 mM glucose at the final concentration indicated. After 15 min at 30 °C under continuous bubbling with $O_2$ and mild shaking, the hemidiaphragms were transferred to 20 ml of fresh KRO buffer containing 5 mM glucose and further incubated for 15 min under the same conditions. Subsequently, the hemidiaphragms were washed briefly with KRO buffer containing 2 mM pyruvate and 5 mM sucrose; they were then incubated in 20 ml of the same buffer supplemented with insulin/PIG-P for 10 min under continuous bubbling with $O_2$ and mild shaking, and then washed with KRO buffer containing 2 mM pyruvate, 1 mM deoxyglucose and 4 mM sucrose. Uptake was initiated by transfer of the diaphragms to 20 ml of KRO buffer containing 2 mM pyruvate, 1 mM 2-[$^3$H]deoxyglucose (25 Ci/mmol; 5 $\mu$Ci) and 4 mM [U-$^{14}$C]sucrose (20 mCi/mmol; 5 $\mu$Ci). After incubation for 20 min under the above conditions, the hemidiaphragms were blotted on filter paper, released from the rib cage, weighed and transferred to scintillation vials. After the addition of 1.5 ml of tissue solubilizer (Biolute S; Zinsser, Frankfurt, Germany), incubation overnight and supplementation with 10 ml of scintillation cocktail (Quickscint 501; Zinsser), $^3$H and $^{14}$C radioactivity was determined by liquid-scintillation counting. To correct for non-specific uptake (entrapment of 2-deoxyglucose in extracellular spaces and diffusion across the membrane), specific uptake was calculated as the difference between the total amount of 2-deoxyglucose and sucrose associated with the diaphragm. Non-specific uptake accounted for 15–25 % of total 2-deoxyglucose associated and did not vary significantly between incubations with insulin and PGI-P. Under these experimental conditions, the specific uptake of 2-deoxyglucose in the basal as well as stimulated state in diaphragm was linear for at least 45 min.

### Two-dimensional analysis of phosphoproteins

$^{33}$P-labelled cardiomyocytes ($5 \times 10^5$) were lysed in buffer containing 50 mM Tris, 150 mM NaCl, 20 mM NaF, 10 mM EDTA, 1 mM $Na_3VO_4$, 0.3 mM PMSF, 2 $\mu$M leupeptin, 2 $\mu$M pepstatin and 1 % (v/v) Triton, pH 7.4. After incubation for 1 h at 4 °C, the suspension was centrifuged at 16000 ***g*** for 2 min and the supernatant subjected to two-dimensional PAGE as described by O'Farrell [23] with modifications. Isoelectric focusing was performed on Immobiline DryStrips (Pharmacia), which exhibit an immobilized pH gradient of 3.0–10.5. Electrophoresis was carried out for 8 h at 300 V and for 10 h at 2 kV. After focusing was complete, strips were subjected to horizontal SDS/PAGE using 10 % gels. Gels were then silver stained, dried and subjected to autoradiography on a Fujix BAS 1000 bio-imaging analyser.

### Immunoblotting

Cardiomyocytes ($2 \times 10^6$) were stimulated with insulin or PIG-P and subsequently incubated in lysis buffer (see above) for 1 h at 4 °C. After centrifugation, the supernatant was subjected to immunoprecipitation with IRS-1 antibody. This was preadsorbed to Protein A/Protein G acrylamide beads for 2 h at 4 °C and was added to the solubilized cell supernatant and incubated for 16 h at 4 °C with gentle rotation. After centrifugation, the immunopellet was washed three times with lysis buffer and twice with PBS. The supernatant of the first immunoprecipitation was subjected to immunoprecipitation with agarose-coupled anti-phosphotyrosine antibody according to the protocol outlined for IRS-1. Immunoprecipitates were then separated by SDS/PAGE using gradient (8–18 %) horizontal gels and transferred to PVDF filters in a semi-dry blotting apparatus [24]. Filters were blocked for 60 min in PBS, pH 7.4, containing 1 % BSA. Thereafter, filters were incubated for 16 h at 4 °C with a 1:1000 dilution of the anti-phosphotyrosine antibody conjugated to alkaline phosphatase. Substrates for alkaline phosphatase were then added for appropriate colour development. Quantification was performed densitometrically using BioImage whole-band analysis software (Millipore, Eschborn, Germany).

### Assay of PI 3-kinase activity

PI 3-kinase activity was measured directly in IRS-1 immunoprecipitates in 50 $\mu$l of reaction mixture containing 0.2 mg/ml phosphatidylinositol, 20 mM Hepes, pH 7.1, 0.4 mM EGTA, 0.4 mM $Na_2HPO_4$ and 10 mM $MgCl_2$ in the absence or presence of wortmannin (1 $\mu$M). The latter completely blocks PI 3-kinase activity and was used for the determination of background activity. The kinase buffer was incubated with the immunoprecipitates for 5 min at room temperature and the reaction was started by the addition of [$\gamma$-$^{32}$P]ATP (40 $\mu$M and 0.1 $\mu$Ci/$\mu$l). After 20 min, the reaction was stopped by the addition of 30 $\mu$l of 4 M HCl and 130 $\mu$l of chloroform/methanol (1:1, v/v). The organic phase was extracted and spotted on a silica-gel TLC plate (Merck) and developed in chloroform/methanol/25 % $NH_4OH$/water (43:38:5:7, by vol.). Plates were dried and subsequently visualized and analysed on a Fujix BAS 1000 bio-imaging analyser.

### Determination of tyrosine phosphorylation of the insulin receptor and IRS-1 and of PI 3-kinase activity in rat adipocytes

Adipocytes ($2.5 \times 10^6$) were incubated with insulin or PIG-P in 10 ml of KRB buffer for 20 min at 37 °C, subsequently separated from the medium by centrifugation and lysed in 1 ml of chilled buffer containing 20 mM Tris/HCl, pH 7.4, 150 mM NaCl, 10 % glycerol, 2 mM EDTA, 1 mM $Na_3VO_4$, 50 mM sodium pyrophosphate, 0.2 mM PMSF, 20 $\mu$g/ml leupeptin, 10 $\mu$g/ml pepstatin and 25 $\mu$g/ml aprotinin by 10 strokes in a loose-fitting Teflon-in-glass homogenizer on ice. The fat-free homogenate, prepared by centrifugation, was supplemented with Triton X-100 (1 % final concentration), incubated for 1 h at 4 °C and finally

centrifuged. The supernatant was incubated with anti-(insulin receptor), anti-IRS-1 or non-immune rabbit IgG antibodies for 3 h at 4 °C and then with Protein A/G–Sepharose overnight at 4 °C. The anti-(insulin receptor) and anti-IgG as well as portions of the anti-IRS-1 immunoprecipitates were subjected to SDS/PAGE and immunoblotted using anti-phosphotyrosine primary monoclonal antibody and the enhanced chemiluminescence detection system. Other portions of the anti-IRS-1 immunoprecipitates were assayed for PI 3-kinase by incubating in 100 $\mu$l of 20 mM Tris/HCl, pH 7.0, containing 50 $\mu$M [$\gamma$-$^{32}$P]ATP (5 $\mu$Ci), 10 mM $MgCl_2$, 2 mM $MnCl_2$, 100 mM NaCl, 2 mM EDTA, 0.5 $\mu$M wortmannin (for control incubations only), 10 $\mu$g of phosphatidylinositol and 1 $\mu$g of phosphatidylserine for 15 min at 22 °C. The reaction was stopped and the products were processed for TLC analysis as outlined above.

### Presentation of data and statistics

All data analysis was performed using Prism (GraphPad, San Diego, CA, U.S.A.) or t-ease (ISI, Philadelphia, PA, U.S.A.) statistical software. Significance of reported differences was evaluated by using the null hypothesis and *t* statistics for paired data. Corresponding significance levels are indicated in the Figures.

## RESULTS

### Kinetics of PIG-P action in isolated adipocytes

We recently demonstrated that PIG-P exerts a wide array of insulin-mimetic actions in isolated rat adipocytes including stimulation of lipogenesis, inhibition of lipolysis, activation of glucose transport, GLUT4 translocation and glycerol phosphate acyltransferase [16]. In order to gain initial insights into the mechanism of PIG-P action, we studied the time course of the onset and duration of glucose-transport activation (Figure 1, top). Incubation of adipocytes with either a half-maximally (2 $\mu$M) or maximally (10 $\mu$M) effective concentration of PIG-P for increasing periods of time before the start of the glucose-transport assay demonstrated maximal activation (3.5- and 6-fold respectively) after 12–17 min with a half-time of 6–8 min. A similar but even more rapid action profile was observed for insulin with a half-time of less than 5 min (Figure 1) in agreement with earlier reports in the literature [25]. Extended incubation periods resulted in a continuous loss of both PIG-P and insulin action. The decline in the glucose-transport rate as a function of time of incubation with both insulin and PIG-P starting after 20 min may be explained by degradation of the agents and/or desensitization of the adipocytes. Preliminary results indicated a half-life for insulin of 30–40 min and for PIG-P of 12–15 min in the adipocyte incubation medium under the routine assay conditions (S. Petry, K. Sauber and G. Müller, unpublished results). Thus prolonged incubation (> 40 min and 20 min respectively) of adipocytes with insulin or PIG-P may cause a reduction in the concentration of functional molecules accounting for about 50 % loss of glucose-transport activation, even considering the reported half-time for inactivation of a fully activated glucose-transport system in isolated rat adipocytes of 8–12 min. TLC purification and gas chromatographic/mass spectral analysis revealed that degradation of PIG-P starts from both termini of the molecule. It thereby loses important structural determinants (opening of the cyclic phosphate residue, removal of the inositol phosphate and tripeptide moieties). The resulting truncated PIG-P has only about 10–15 % of the insulin-mimetic activity left. However, the rapid approx. 30 % decline in glucose-transport activation between 20 and 45 min can hardly be explained by loss

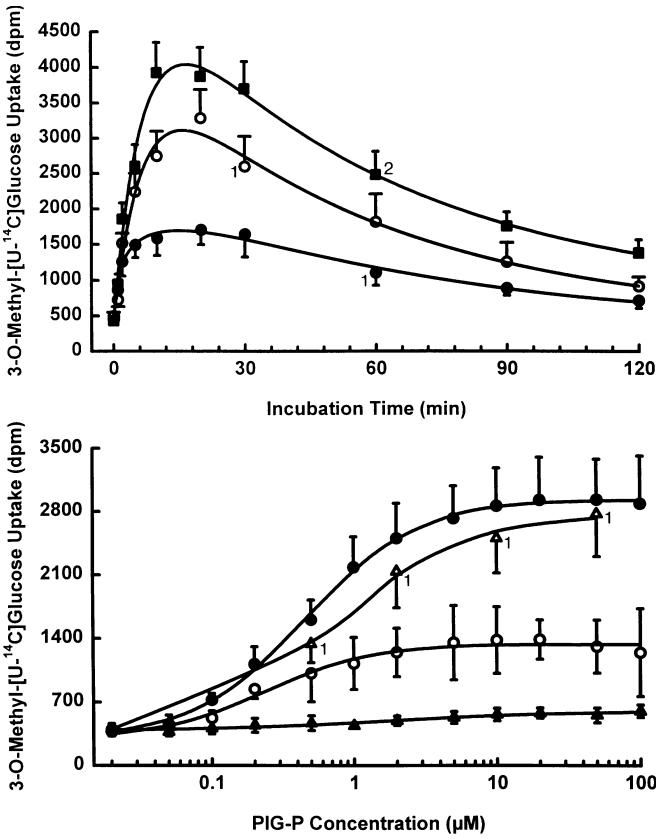


**Figure 1 Time course of onset and reversibility of PIG-P action on glucose transport in isolated adipocytes**

Top: rat adipocytes were incubated at 37 °C with 2 $\mu$M (●) or 10 $\mu$M (○) PIG-P or 10 nM (■) insulin for increasing lengths of time before the start of the 3-*O*-methylglucose-transport assay, which was initiated by the addition of 3-*O*-methyl-[U-$^{14}$C]glucose (50 $\mu$M final concentration). Transport was terminated and quantified as outlined in the Materials and methods section. Each point represents the mean ± S.D. from four different adipocyte preparations with incubations and glucose-transport assays in quadruplicate. Significant difference from corresponding 20 min incubation is indicated: $^1P = 0.05$ and $^2P = 0.01$. Bottom: adipocytes were incubated with 10 $\mu$M PIG-P for 15 min. Portions of the cells were assayed for 3-*O*-methylglucose transport either immediately after the incubation (●) or immediately (△), 5 min (○) or 15 min (▲) after three washing cycles of the cells. Each point represents the mean ± S.D. from three different adipocyte preparations with incubations and glucose transport assays in duplicate. [1]Not significantly different from control (●) at $P > 0.05$.

of functional insulin or PIG-P from the incubation medium. It is conceivable that activation of the glucose-transport system by either insulin or PIG-P to about 70–100 % of maximum for a prolonged time (> 20 min) causes its desensitization to either compound, perhaps in order to protect the adipocytes against high intracellular glucose in terms of the glucose toxicity concept. This mechanism may be similar to the desensitization of isolated adipocytes to insulin activation of the receptor in the presence of high glucose and insulin already observed after 1 h. In line with these explanations is our recent finding that the addition of a second portion of insulin or PIG-P to adipocytes 20 min after the first stimulation with either compound did not prevent the initial phase of rapid decline (at 20 min) but caused a considerable delay of the following phase of transport inactivation (results not shown).

As shown in Figure 1 (bottom), PIG-P signalling is very rapidly reversed and completely terminated on removal of PIG-

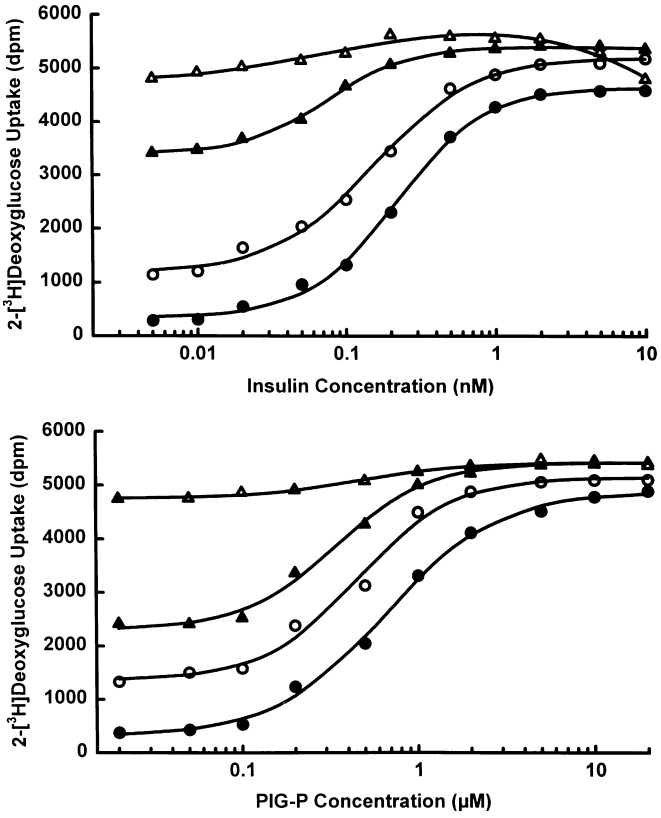


**Figure 2 Effect of PIG-P on insulin-stimulated glucose transport in adipocytes**

Adipocytes were incubated for 20 min with various concentrations of PIG-P (●, 0; ○, 0.2 $\mu$M; ▲, 1 $\mu$M; △, 10 $\mu$M) in the presence of increasing concentrations of insulin (top) or with various concentrations of insulin (●, 0; ○, 0.1 nM; ▲, 1 nM; △, 10 nM) in the presence of increasing concentrations of PIG-P (bottom) before the start of the glucose-uptake assay using 2-deoxy-D-[$^3$H]glucose. Uptake was terminated after 5 min and quantified as described in the Materials and methods section. Data are mean values from two independent adipocyte preparations with incubations and glucose-transport assays in quadruplicate.

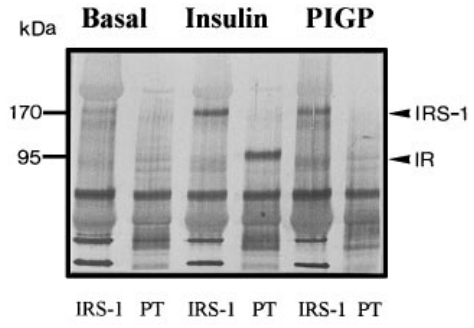


**Figure 3 Effect of PIG-P on the tyrosine phosphorylation of IRS-1**

Cardiomyocytes ($2 \times 10^6$) were incubated for 5 min with either insulin (350 nM) or PIG-P (2 $\mu$M). Cell extracts were subjected to a two-step immunoprecipitation protocol using IRS-1 antibody (IRS-1) followed by agarose-coupled anti-phosphotyrosine antibody (PT), with the latter being added to the supernatant of the first immunoprecipitation. Immunopellets were then analysed by SDS/PAGE and immunoblotted with anti-phosphotyrosine monoclonal antibodies. Signals were visualized using the alkaline phosphatase reaction. IR, location of the 95 kDa $\beta$-subunit of the insulin receptor. One representative experiment of three is shown.

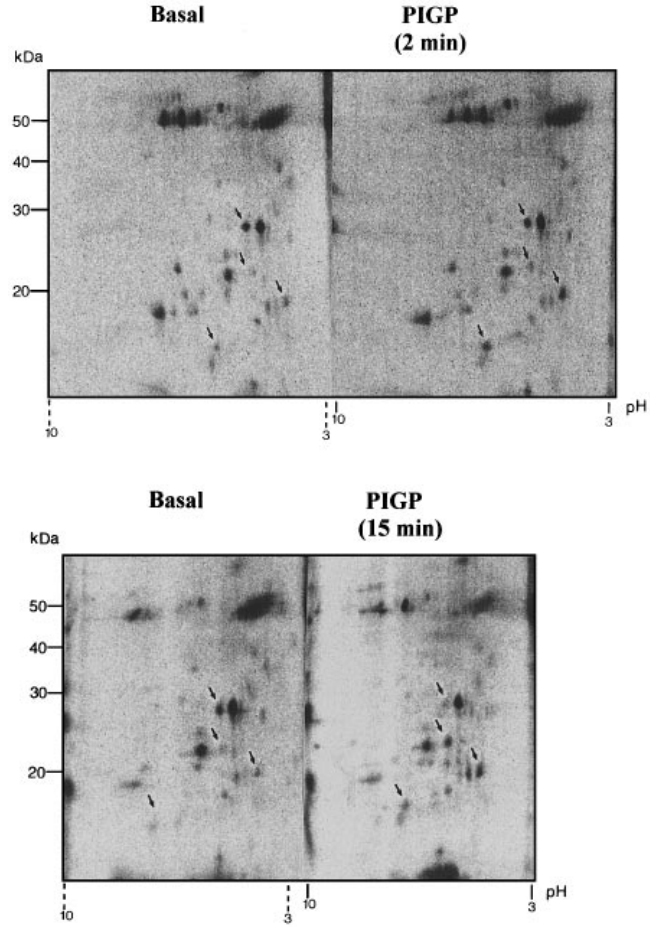


**Figure 4 Two-dimensional analysis of $^{33}$P-labelled phosphoproteins in cardiomyocytes treated with PIG-P**

Cardiomyocytes ($5 \times 10^5$) were labelled with [$^{33}$P]$P_i$ (200 $\mu$Ci) for 2.5 h. Cells were then incubated in the absence or presence of PIG-P (2 $\mu$M) for 2 (top) or 15 (bottom) min. Cell extracts were subjected to isoelectric focusing followed by SDS/PAGE, as detailed in the Materials and methods section. Gels were stained, dried and subjected to autoradiography on a Fujix BAS 1000 bio-imaging analyser. One representative autoradiogram from three independent experiments is shown in each case. Arrows indicate proteins reproducibly modified by PIG-P.

P from the incubation medium. After three washing cycles, a 5 min incubation of adipocytes in the absence of PIG-P (the washing resulted in a 1000-fold dilution of PIG-P) induced a 70% decrease in the response at each PIG-P concentration compared with control cells. After 15 min, no glucose-transport activation was left (Figure 1, bottom).

PIG-P and insulin were found to stimulate cardiac glucose transport in a non-additive fashion at maximal effective concentrations [16]. This relationship has now been investigated in more detail using isolated adipocytes. Simultaneous incubation with a constant concentration of PIG-P and increasing insulin concentrations (Figure 2, top) or with a constant insulin concentration and increasing concentrations of PIG-P (Figure 2, bottom) resulted in additive effects at submaximal and non-additive effects at maximal PIG-P (10 $\mu$M) and insulin (10 nM) concentrations respectively. In the presence of insulin or PIG-P the dose–response curves became flat resulting in largely reduced stimulation factors for glucose-transport activation. The observed non-additive effects when glucose transport exceeds a

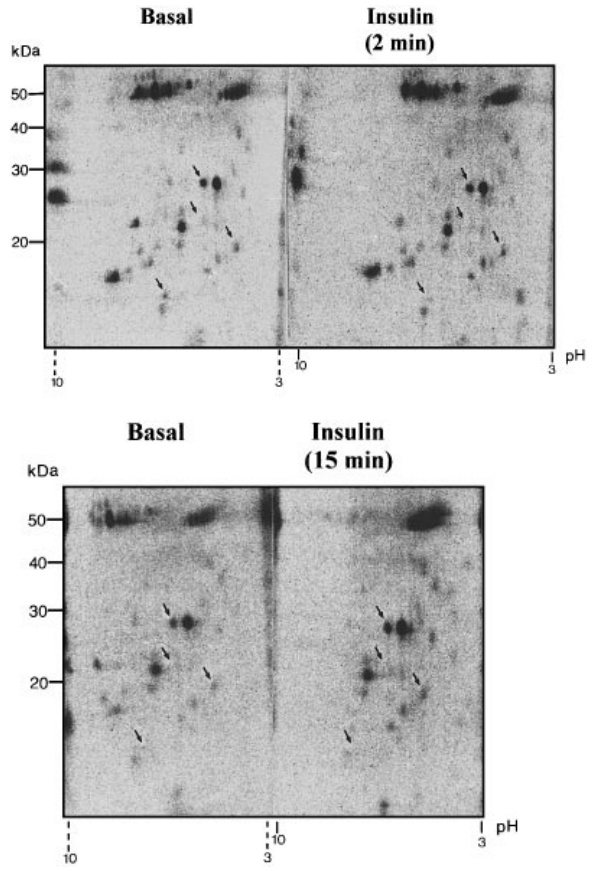


**Figure 5 Two-dimensional analysis of $^{33}$P-labelled phosphoproteins in cardiomyocytes treated with insulin**

Cardiomyocytes were labelled with [$^{33}$P]$P_i$ and subsequently incubated with insulin (350 nM) for 2 and 15 min. Two-dimensional PAGE was then performed as described in the legend to Figure 4.

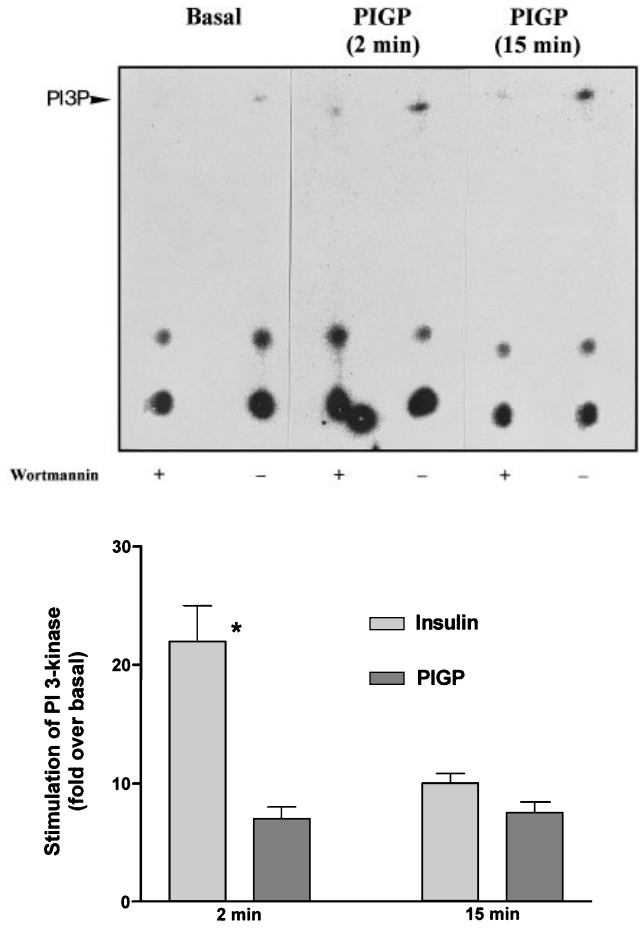


**Figure 6 Effect of PIG-P on IRS-1-associated PI 3-kinase activity**

Top: cardiomyocytes ($2 \times 10^6$) were stimulated with PIG-P (2 $\mu$M), and PI 3-kinase was co-immunoprecipitated with anti-IRS-1 antibodies, as outlined in the Materials and methods section. Kinase reaction was then performed in the absence or presence of wortmannin (1 $\mu$M), and lipid products were separated by TLC followed by autoradiography. Bottom: Quantification of autoradiograms was performed with a bio-imaging analyser and PI 3-kinase activity is expressed as fold stimulation over basal. Data were corrected for non-specific kinase activity determined in the presence of wortmannin. The data represent mean values $\pm$ S.E.M. from three separate experiments. * Significantly different from stimulation with PIG-P, $P = 0.05$.

certain threshold value and the upper limit for glucose-transport activation by a combination of PIG-P and insulin make it likely that PIG-P uses part of the insulin signalling cascade to produce its insulin-mimetic effects.

### Effects of PIG-P on the phosphoprotein pattern in isolated cardiomyocytes

Tyrosine phosphorylation of IRS-1 by the insulin receptor kinase has been recognized as representing an immediate early step of insulin signalling [1,3]. We therefore investigated, using freshly isolated rat cardiomyocytes, whether this segment of the insulin signalling cascade is modified by PIG-P and whether additional phosphoproteins are affected by the mediator. These cells are highly responsive to insulin and PIG-P [16] and can be efficiently labelled with [$^{33}$P]$P_i$ to enable phosphoprotein analysis [26]. In a first series of experiments tyrosine phosphorylation was determined by Western-blot analysis of IRS-1 and phosphotyrosine immunoprecipitates from cardiomyocytes subjected to short-term (5 min) stimulation with insulin or 2 $\mu$M PIG-P, a concentration that was almost maximally effective in inducing glucose transport in both isolated cardiomyocytes and adipocytes [16] (Figure 3). As expected, insulin markedly enhanced the tyrosine phosphorylation of IRS-1 and of a 95 kDa phosphoprotein previously identified as the insulin receptor $\beta$-subunit [26]. PIG-P was essentially unable to induce autophosphorylation of the insulin receptor. However, the compound increased the tyrosine phosphorylation of IRS-1, exhibiting $50 \pm 8\,\%$ of the stimulatory potency of the hormone under the same experimental conditions (Figure 3). This striking observation indicates that PIG-P is able to mimick insulin signalling at the level of IRS-1 despite by-passing the insulin receptor. This interpretation is compatible with our previous finding [16] that PIG-P is able to exert insulin-mimetic effects in adipocytes depleted of functional insulin receptors.

Further dissection of insulin and PIG-P signalling was then achieved by performing two-dimensional PAGE of phosphoproteins detectable after short-term (2.5 h) labelling of cardiomyocytes with [$^{33}$P]$P_i$. Basal and PIG-P-treated cell extracts were always run within the same gel to establish reproducible run conditions. Significant differences in the phosphoprotein pattern only became detectable in the low-molecular-mass ($< 50$ kDa) range. As can be seen from the representative autoradiogram shown in Figure 4, three phosphoproteins with molecular masses

**Table 1 Effect of PIG-P on the tyrosine phosphorylation of the insulin receptor and IRS-1 and on the activity of PI 3-kinase in rat adipocytes**

Isolated rat adipocytes were incubated in the absence or presence of increasing concentrations of insulin or PIG-P for 20 min at 37 °C. Total cell lysates were subjected to immunoprecipitation with either anti-(insulin receptor) or anti-IRS-1 antibodies. The immunoprecipitates were separated by SDS/PAGE and analysed for phosphotyrosine by Western blotting and subsequent immunodecoration with anti-phosphotyrosine antibodies. Phosphotyrosine-containing polypeptides were visualized using enhanced chemiluminescence, which was quantitatively evaluated by direct luminometry. Portions of the anti-IRS-1 immunoprecipitates were used for determination of PI 3-kinase activity in the absence or presence of 0.5 $\mu$M wortmannin. The tyrosine-phosphorylation state of the insulin receptor and IRS-1 as well as the activity of PI 3-kinase in the basal state were set at 100 arbitrary units. The IRS-1-associated PI 3-kinase activity was corrected for non-specific activity not inhibited by wortmannin. The results represent means ± S.D. from three different adipocyte preparations with activity determinations in quadruplicate. Values that are significantly different from basal are indicated: $^{*}P = 0.05$; $^{**}P = 0.02$; $^{***}P = 0.01$; †$P = 0.005$; ††$P = 0.002$; †††$P = 0.001$.

| | Tyrosine phosphorylation | | |
|---|---|---|---|
| Activator | Insulin receptor | IRS-1 | IRS-1-associated PI 3-kinase activity |
| None | 100 ± 27 | 100 ± 15 | 100 ± 34 |
| Insulin (nM) | | | |
| 0.01 | 112 ± 20 | 95 ± 22 | 109 ± 28 |
| 0.1 | 139 ± 17* | 169 ± 30* | 121 ± 19 |
| 0.3 | 181 ± 44** | 278 ± 69*** | 149 ± 25* |
| 1 | 281 ± 58*** | 393 ± 104† | 192 ± 40** |
| 3 | 370 ± 65†† | 488 ± 94† | 275 ± 63*** |
| 10 | 397 ± 73††† | 529 ± 111†† | 301 ± 92† |
| PIG-P ($\mu$M) | | | |
| 0.1 | 97 ± 12 | 102 ± 10 | 95 ± 13 |
| 0.2 | 92 ± 8 | 134 ± 12* | 123 ± 11* |
| 0.5 | 109 ± 14 | 188 ± 28** | 163 ± 33** |
| 1 | 103 ± 19 | 220 ± 37*** | 196 ± 29*** |
| 3 | 110 ± 17 | 238 ± 49*** | 218 ± 34*** |
| 10 | 119 ± 22 | 249 ± 40*** | 229 ± 37*** |

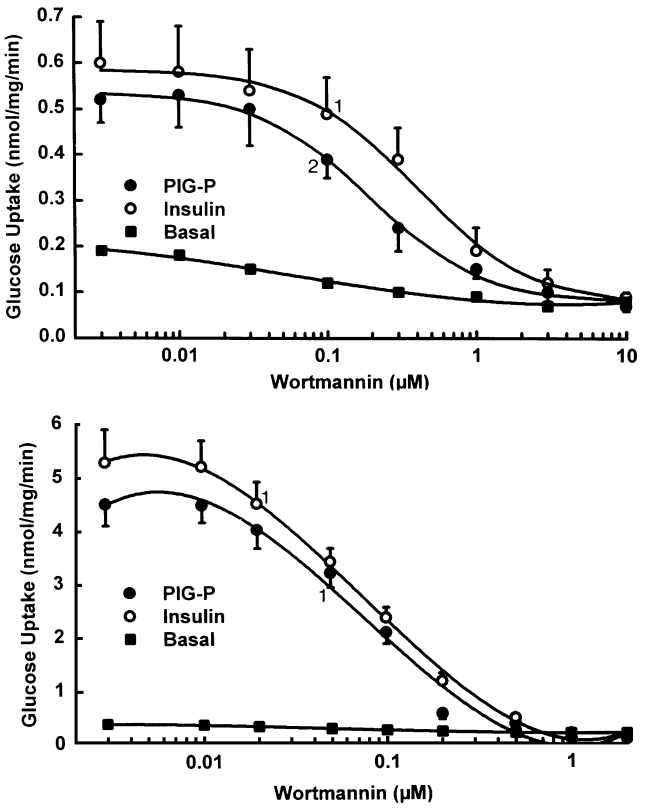


**Figure 7 Wortmannin inhibits stimulation of glucose uptake by PIG-P in rat diaphragms and adipocytes**

Rat diaphragms (top) or isolated rat adipocytes (bottom) were incubated with the indicated concentrations of wortmannin for 5 min at 37 °C before the addition of insulin (final concentration 10 nM for adipocytes; 300 nM for diaphragms; ○) or PIG-P (5 $\mu$M for adipocytes; 20 $\mu$M for diaphragms; ●). After 15 min of incubation the adipocytes and diaphragms were assayed for glucose-uptake as outlined in Figure 2. Each point represents the mean ± S.D. from at least three independent experiments with determinations in quadruplicate. Significant difference from control is indicated: $^{1}P = 0.05$ and $^{2}P = 0.02$.

of about 15, 20 and 24 kDa were rapidly phosphorylated in response to PIG-P after both 2 (top) and 15 (bottom) min. In addition, PIG-P induced the time-dependent dephosphorylation of a 30 kDa phosphoprotein with near-complete dephosphorylation after 15 min of PIG-P incubation (Figure 4, bottom). Cardiomyocytes were then labelled with [$^{33}$P]$P_i$, incubated with insulin, and subjected to the analysis outlined above. As illustrated in Figure 5, insulin completely failed to modify the phosphoproteins regulated in response to PIG-P (compare with Figure 4, top).

### Effect of PIG-P on signalling pathways downstream of IRS-1

The data so far suggest that the insulin-mimetic activity of PIG-P could result from the enhanced tyrosine phosphorylation of IRS-1 induced by the PIG-P compound. It is well established that PI 3-kinase represents an essential element of the diversification and further downstream propagation of the insulin signal to the insulin-responsive glucose transporter GLUT4 [4,5]. We therefore analysed whether PIG-P action might be accompanied by an increase in the IRS-1-associated PI 3-kinase activity. Representative TLC phosphoimages of PI 3-kinase activity obtained from IRS-1 immunoprecipitates of basal and PIG-P-treated cells are presented in Figure 6 (top). After both 2 and 15 min a marked increase in the enzyme activity (7-fold) could be detected. At 2 min, insulin action on PI 3-kinase activity was much more pronounced than PIG-P action; however, this insulin action declined with extended incubation times (15 min) whereas PIG-P action remained stable under these conditions (Figure 6, bottom) reaching about 50 % of the stimulatory effect of insulin.

The described effects of PIG-P on the tyrosine phosphorylation state of the insulin receptor and IRS-1 as well as on the activity of PI 3-kinase in rat cardiomyocytes were confirmed with isolated rat adipocytes (Table 1). Whereas insulin caused a concentration-dependent increase in tyrosine phosphorylation of the insulin receptor with a 4-fold maximal stimulation (at 10 nM), PIG-P did not elicit any statistically significant phosphate incorporation into the receptor, even at 10 $\mu$M which induced 70 % of the glucose-transport activation of insulin. In contrast, tyrosine phosphorylation of IRS-1 and activation of IRS-1-associated PI 3-kinase were significantly enhanced by both insulin and PIG-P in a concentration-dependent manner. PIG-P-induced tyrosine phosphorylation of IRS-1 and activation of PI 3-kinase approach 44 and 76 % respectively of the maximal insulin effect, corresponding to a 2.3-fold stimulation in both cases. No significant tyrosine phosphorylation or PI 3-kinase activity could be detected in control IgG immunoprecipitates.

In order to elucidate whether the activation of PI 3-kinase by PIG-P is indeed functionally linked to glucose-transport activation by the compound, we used the specific PI 3-kinase inhibitors, wortmannin and LY294002 [27]. As presented in

Figure 7, a 5 min preincubation with wortmannin produced a dose-dependent inhibition of glucose-transport activation by both PIG-P and insulin in diaphragms and adipocytes. In both tissues a very similar sensitivity of insulin and PIG-P action towards wortmannin could be detected, with complete inhibition at 0.2–1 $\mu$M (Figure 7). Nearly identical results were observed with the highly specific PI 3-kinase inhibitor LY249002 (maximum inhibition at 100 $\mu$M for diaphragm and adipocytes; results not shown). Essentially no inhibition of glucose-transport activation by insulin and PIG-P in diaphragms and adipocytes was found after preincubation with the S6 kinase inhibitor rapamycin [28] and the mitogen-activated protein kinase inhibitor PD098059 [2].

## DISCUSSION

Considerable evidence supports the notion of an insulin-mediated activation of a specific phospholipase C leading to the generation of soluble PIG molecules [7–9,11] from free glycolipids or GPI membrane protein anchors [15]. Glycan mediators have been partially purified from different sources including $BC_3H1$ cells [29], T-cells [30] and liver membranes [31]; however, undefined chemical structures of these compounds did not allow the precise analysis of molecular signalling pathways. Two earlier investigations reported on the action profile of structurally defined inositol glycan phosphates obtained from either the GPI anchor of *Trypanosoma brucei* variant surface glycoprotein [15] or the GPI anchor of human erythrocyte acetylcholinesterase [32]. The former mediator inhibits isoprenaline-stimulated lipolysis in adipocytes and gluconeogenesis in hepatocytes [15], whereas the latter compound was shown to antagonize glucagon-activated phosphorylase activity in liver cells [32]. We recently reported on an additional completely characterized PIG compound that was obtained by sequential cleavage of the GPI-anchored protein, Gce1p, from the yeast *S. cerevisiae* [16]. The glycan core structure of this molecule is very similar to the above-mentioned mediators [15,32], but it contains a tripeptide with the following structure: Tyr-Cys-Asn-ethanolamine-$PO_4$-glycan. On the other hand, the mediators from *T. brucei* and human erythrocytes contain only a single amino acid, Asp [15] and Gly [32] respectively. In contrast with all other insulin-mimetic PIG compounds, the PIG-P from yeast potently activates GLUT4 translocation and glucose transport in muscle and fat [16]. It was therefore of major interest to study the signalling pathways of PIG-P leading to glucose-transport activation and to elucidate its relationship to signalling intermediates involved in the action of insulin.

The similar kinetics of onset and deactivation of PIG-P and insulin action on glucose transport in isolated adipocytes, as presented in this paper, as well as the additive and non-additive effects of the two agents on glucose transport observed at submaximal and maximal concentrations respectively, support the assumption that PIG-P uses some steps of the insulin signalling cascade. The concentrations required for maximum PIG-P action are in excellent agreement with the data of Deeg et al. [32], who used a chemically defined PIG from human erythrocytes, but are significantly lower than those reported by Misek and Saltiel [15] for a homogeneous PIG structure from *T. brucei*. PIG-P action on glucose transport exhibits marked reversibility (Figure 1, bottom) with even more rapid termination of the signal than insulin [25]. These data suggest that PIG-P signalling may be initiated at the cell surface and that sustained signalling requires the continuous presence of the compound.

A key finding of the present investigation is in the observation of markedly enhanced rapid tyrosine phosphorylation of IRS-1 in response to PIG-P in isolated rat cardiomyocytes and adipocytes. This effect agrees with the rapid stimulation of glucose transport in these cells by the glycan [16]. The kinase(s) or phosphatase(s) mediating this effect has still to be identified, but we have clearly excluded the involvement of the insulin receptor in this process. It has now been recognized that tyrosine phosphorylation of IRS-1 is not limited to tyrosine kinase receptors, but can also be mediated by growth hormone and cytokine receptors [33–35]. More recently, agonists binding to G-protein-coupled receptors, such as angiotensin II [36] and gastrin [37], were also shown to induce tyrosine phosphorylation of IRS-1. These ligands activate cytosolic kinases of the Janus kinase family, which subsequently associate with and phosphorylate IRS-1 [38]. It may be speculated that PIG-P binds to one of these receptors leading to the observed tyrosine phosphorylation of IRS-1. Alternatively, it is interesting to note that a variety of GPI-anchored proteins like Thy-1 are known to associate with non-receptor tyrosine kinases of the Src family [39]. The dual acylated version of these kinases partition into the inner leaflet of the plasma membrane forming so-called detergent-insoluble complexes, in close association with GPI-anchored proteins and glycolipids [40]. The following lines of evidence hint at a role for these structures in mediating signalling by GPI or PIG molecules. (1) In T-cells and neutrophils, cross-linking of certain GPI-anchored proteins with antibodies activates non-receptor tyrosine kinases, including Src, and elicits cell-specific responses [41]. (2) Caveolin, a resident protein of detergent-insoluble complexes, was found to be phosphorylated at tyrosine residues on stimulation of 3T3-L1 adipocytes with insulin [42]. (3) Concentration-dependent phosphorylation of caveolin in detergent-insoluble complexes was observed after treatment of isolated rat adipocytes with exogenous bacterial phosphatidylinositol-specific phospholipase C [43]. (4) A GPI anchor alone was shown to induce rapid onset of tyrosine phosphorylation [44].

The mechanism by which the Src family of tyrosine kinases interact with GPI-anchored proteins remains unclear. We suggest the following working hypothesis. GPI-anchored proteins and free GPI lipids interact via certain determinants within their glycan core (and C-terminal protein portion respectively) with an as yet unidentified transmembrane 'bridge' protein of the detergent-insoluble complexes. This protein (possibly caveolin) is also in contact with the Src kinases via the fatty acyl chains and certain protein epitopes of the latter. Cross-linking of GPI-anchored proteins with antibodies (as shown for T-cells and neutrophils) or dissociation of GPI structures from the 'bridge' protein by competition with excess GPI anchors or soluble PIG(-P) molecules (as putatively performed in the present study) will result in a conformational change in the 'bridge' protein leading to activation of the associated tyrosine kinase. The PIG-P derived from Gce1p of *S. cerevisiae* may be particularly efficient in interacting with the 'bridge' protein in comparison with other PIG structures or GPI anchors. At present we are trying to identify the putative 'bridge' protein by affinity cross-linking to photoreactive PIG-P probes.

In an earlier study, Witters et al. [45] found that a PIG-related substance, released into conditioned medium of insulin-stimulated hepatoma cells and resembling phospholipase C-digested material, stimulated protein phosphorylation in isolated rat adipocytes. Romero et al. [46] reported selective blockade of insulin-stimulated protein phosphorylation in intact $BC_3H1$ cells by anti-inositolglycan antibodies. Mato and co-workers [14] showed that both insulin and PIG molecules, prepared by phospholipase C treatment of rat liver membranes, reduced the isoprenaline-dependent serine phosphorylation of phospholipid methyltransferase in isolated rat adipocytes. Furthermore, Alemany et al. [47] showed that a PIG purified from rat liver

membranes was able to mimick several phosphorylation and dephosphorylation reactions produced by insulin in isolated rat adipocytes. More recently, Misek and Saltiel [48] reported that the structurally characterized PIG from *T. brucei* was able to attenuate the isoprenaline-induced phosphorylation of a 70 kDa protein in rat adipocytes in a manner comparable with that of insulin. Using two-dimensional analysis of whole-cell extracts, we show here that PIG-P was able to promote the dephosphorylation of a 30 kDa protein in cardiomyocytes. Furthermore, three additional proteins of 15, 20 and 24 kDa rapidly became phosphorylated in response to the PIG-P. However, insulin completely failed to induce these protein modifications. This differs from the studies cited above [47,48] on protein phosphorylation in response to PIG structures and insulin and may indicate that PIG-P is not generated in response to insulin, at least not in the cardiomyocyte. This assumption is supported by unaltered tyrosine phosphorylation of IRS-1 and association of PI 3-kinase in GPI-defective cells despite the absolute requirement of GPI synthesis for the stimulation of glycogen synthesis by insulin [49]. We therefore conclude that PIG-P is not an endogenous mediator of insulin action but a powerful mimicker of the hormone by (a) triggering tyrosine phosphorylation of IRS-1 and downstream signalling (see below), and (b) regulating intracellular metabolism by activating protein phosphatases [50].

Tyrosine-phosphorylated IRS-1 is of major importance for the docking of downstream signalling elements leading to the diversification of insulin action [1–3]. Interaction of IRS-1 with the p85 regulatory subunit of PI 3-kinase and activation of this enzyme has now been recognized to represent an essential requirement for the activation of glucose transport by insulin [4,5]. We have confirmed for both cardiomyocytes and adipocytes that PIG-P-induced tyrosine phosphorylation of IRS-1 is accompanied by significant stable activation of IRS-1-associated PI 3-kinase activity (Figure 6, Table 1). In the myocytes at 2 min, the effect of insulin on PI 3-kinase activity was much stronger (20-fold compared with 7-fold), most probably reflecting the different upstream kinases and a differential phosphorylation pattern of IRS-1. The functional implication of PI 3-kinase activation for PIG-P-stimulated glucose transport in muscle and adipose tissue was confirmed by using the PI 3-kinase inhibitors wortmannin and LY294002. Our data show dose-dependent complete inhibition of PIG-P-activated glucose transport in both tissues with an identical result obtained for insulin. Activation of PI 3-kinase *per se* is not sufficient to stimulate glucose transport. Instead, recruitment of the activated enzyme to a specific compartment may be an important prerequisite for coupling to the glucose transporter [51]. Whereas limited glucose-transport activation can be obtained by drastic overexpression of PI 3-kinase in transfected 3T3-L1 adipocytes [52], the PIG-P-induced increase in glucose transport and GLUT4 translocation (up to 70 % of the maximal insulin effect) [16] was accompanied by a modest stimulation of PI 3-kinase. This suggests that PIG-P, in addition to PI 3-kinase activation, may induce targeting of this enzyme to the same subcellular compartment as insulin, presumably the low-density microsomes. Stimulation of glucose transport and GLUT4 translocation by PIG-P [16] can therefore be explained by an insulin-like activation of the IRS-1/PI 3-kinase pathway by this compound.

In summary, PIG-P represents a powerful mimicker of insulin action in muscle and adipose tissue including glucose transport and all major pathways of carbohydrate and lipid metabolism. We suggest that this compound is not generated as a physiological mediator of insulin action in primary target cells. Instead, PIG-P may harbour all structural requirements needed for insulin signalling independent of the insulin receptor, making it potentially interesting for the treatment of insulin resistance and other diseases.

This work was supported by the Ministerium für Wissenschaft und Forschung des Landes Nordrhein-Westfalen, the Bundesministerium für Gesundheit, the Deutsche Forschungsgemeinschaft (SFB 351 C2), EU COST Action B5 and by a grant from Hoechst Marion Roussel Deutschland GmbH, Frankfurt, Germany.

## REFERENCES


1 White, M. F. and Kahn, C. R. (1994) J. Biol. Chem. **269**, 1–4
2 Saltiel, A. R. (1996) Am. J. Physiol. **270**, 375–385
3 Cheatham, B. and Kahn, C. R. (1995) Endocr. Rev. **16**, 117–142
4 Okada, T., Kawano, Y., Sakakibara, T., Hazeki, O. and Ui, M. (1994) J. Biol. Chem. **269**, 3568–3573
5 Clarke, J. F., Young, P. W., Yonezawa, K., Kasuga, M. and Holman, G. D. (1994) Biochem. J. **300**, 631–635
6 Liscovitch, M. and Cantley, L. C. (1995) Cell **81**, 659–662
7 Vila, M. C., Milligan, G., Standaert, M. L. and Farese, R. V. (1990) Biochemistry **29**, 8735–8740
8 Farese, R. V., Standaert, M. L., Yamada, K., Huang, L. C., Zhang, C., Cooper, D. R., Wang, Z., Yang, Y., Suzuki, S., Toyota, T. and Larner, J. (1994) Proc. Natl. Acad. Sci. U.S.A. **91**, 11040–11044
9 Saltiel, A. R. (1990) Diabetes Care **13**, 244–256
10 Varela-Nieto, I., Leon, Y. and Caro, H. N. (1996) Comp. Biochem. Physiol. **115B**, 223–241
11 Low, M. G. and Saltiel, A. R. (1988) Science **239**, 268–275
12 Shashkin, P. N., Shashkina, E. F., Fernqvist-Forbes, E., Zhou, Y.-P., Grill, V. and Katz, A. (1997) Diabetologia **40**, 557–563
13 Saltiel, A. R. and Sorbara-Cazan, L. R. (1987) Biochem. Biophys. Res. Commun. **149**, 1084–1092
14 Kelly, K. L., Merida, I., Wong, E. H. A., DiCenzo, D. and Mato, J. M. (1987) J. Biol. Chem. **262**, 15285–15290
15 Misek, D. E. and Saltiel, A. R. (1992) J. Biol. Chem. **267**, 16266–16273
16 Müller, G., Wied, S., Crecelius, A., Kessler, A. and Eckel, J. (1997) Endocrinology **138**, 3459–3475
17 Müller, G., Schubert, K., Fiedler, F. and Bandlow, W. (1992) J. Biol. Chem. **267**, 25337–25346
18 Rodbell, M. (1964) J. Biol. Chem. **239**, 375–380
19 Eckel, J., Pandalis, G. and Reinauer, H. (1983) Biochem. J. **212**, 385–392
20 Russ, M. and Eckel, J. (1995) Biochim. Biophys. Acta **1265**, 73–78
21 Kipnis, D. M. and Cori, C. F. (1957) J. Biol. Chem. **224**, 681–693
22 Foley, J. E. and Gliemann, J. (1981) Biochim. Biophys. Acta **648**, 100–106
23 O'Farrell, P. H. (1975) J. Biol. Chem. **250**, 4007–4021
24 Wichelhaus, A., Russ, M., Petersen, S. and Eckel, J. (1994) Am. J. Physiol. **267**, H548–H555
25 Karnieli, E., Zarnowski, M. J., Hissin, P. J., Simpson, I. A., Salans, L. B. and Cushman, S. W. (1981) J. Biol. Chem. **256**, 4772–4777
26 Kolter, T., Uphues, I. and Eckel, J. (1997) Am. J. Physiol. **273**, E59–E67
27 Vlahos, C. J., Matter, W. F., Hui, K. Y. and Brown, R. F. (1994) J. Biol. Chem. **269**, 5241–5248
28 Kuo, C. J., Chung, J., Florentino, D. F., Flanagan, W. M., Blenis, J. and Crabtree, G. R. (1992) Nature (London) **358**, 70–73
29 Suzuki, S., Sugawara, K., Satoh, Y. and Toyota, T. (1991) J. Biol. Chem. **266**, 8115–8121
30 Gaulton, G. N. (1991) Diabetes **40**, 1297–1304
31 Saltiel, A. R. (1987) Endocrinology **120**, 976–972
32 Deeg, M. A., Brass, E. P. and Rosenberry, T. L. (1993) Diabetes **42**, 1318–1323
33 Johnston, J. A., Wang, L.-M., Hanson, E. P., Sun, X.-J., White, M. F., Oakes, S. A., Pierce, J. H. and O'Shea, J. J. (1995) J. Biol. Chem. **270**, 28527–28530
34 Argetsinger, L. S., Hsu, G. W., Myers, Jr., M. G., Billestrup, N., White, M. F. and Carter-Su, C. (1995) J. Biol. Chem. **270**, 14685–14692
35 Uddin, S., Yenush, L., Sun, X.-J., Sweet, M. E., White, M. F. and Platanias, L. C. (1995) J. Biol. Chem. **270**, 15938–15941
36 Saad, M. J. A., Velloso, L. A. and Carvalho, C. R. O. (1995) Biochem. J. **310**, 741–744
37 Kowalski-Chauvel, A., Pradayrol, L., Vaysse, N. and Seva, C. (1996) J. Biol. Chem. **271**, 26356–26361
38 Velloso, L. A., Folli, F., Sun, X. J., White, M. F., Saad, M. J. A. and Kahn, C. R. (1996) Proc. Natl. Acad. Sci. U.S.A. **93**, 12490–12495
39 Thomas, P. M. and Samelson, L. E. (1992) J. Biol. Chem. **267**, 12317–12322
40 Rodgers, W., Crise, B. and Rose, J. K. (1994) Mol. Cell. Biol. **14**, 5384–5391
41 Su, B., Waneck, G. L., Flavell, R. A. and Bothwell, A. L. M. (1991) J. Cell Biol. **112**, 377–384
42 Mastik, C. C., Brady, M. J. and Saltiel, A. R. (1995) J. Cell Biol. **129**, 1523–1531

43 Müller, G. and Geisen, K. (1996) Horm. Metab. Res. **28**, 469–487
44 Tachado, S. D. and Schofield, L. (1994) Biochem. Biophys. Res. Commun. **205**, 984–991
45 Witters, L. A., Watts, T. D., Gould, G. W., Lienhard, G. E. and Gibbs, E. M. (1988) Biochem. Biophys. Res. Commun. **153**, 992–998
46 Romero, G., Gaumez, G., Huang, C. C., Lilley, K. and Luttrell, L. (1990) Proc. Natl. Acad. Sci. U.S.A. **87**, 1476–1480
47 Alemany, S., Mato, J. M. and Stralfors, P. (1987) Nature (London) **330**, 77–79
48 Misek, D. E. and Saltiel, A. R. (1994) Endocrinology **135**, 1869–1876
49 Lazar, D. F., Knez, J. J., Medof, M. E., Cuatrecasas, P. and Saltiel, A. R. (1994) Proc. Natl. Acad. Sci. U.S.A. **91**, 9665–9669
50 Larner, J. (1987) Diabetes **37**, 262–273
51 Nave, B. T., Haigh, R. J., Hayward, A. C., Siddle, K. and Shepherd, P. (1996) Biochem. J. **318**, 55–60
52 Katagiri, H., Asano, T., Ishihara, H., Inukai, K., Shibasaki, Y., Kikuchi, M., Yazaki, Y. and Oka, Y. (1996) J. Biol. Chem. **271**, 16987–16990

Received 18 July 1997/25 September 1997; accepted 9 October 1997